# A 10-Year Radar-Based Climatology of Mesoscale Convective System Archetypes and Derechos in Poland

ARTUR SUROWIECKI

*Department of Climatology, University of Warsaw, and Skywarn Poland, Warsaw, Poland*

MATEUSZ TASZAREK

*Department of Meteorology and Climatology, Adam Mickiewicz University, Poznań, Poland, and National Severe Storms Laboratory, Norman, Oklahoma, and Skywarn Poland, Warsaw, Poland*

(Manuscript received 29 December 2019, in final form 3 May 2020)

ABSTRACT

In this study, a 10-yr (2008–17) radar-based mesoscale convective system (MCS) and derecho climatology for Poland is presented. This is one of the first attempts of a European country to investigate morphological and precipitation archetypes of MCSs as prior studies were mostly based on satellite data. Despite its ubiquity and significance for society, economy, agriculture, and water availability, little is known about the climatological aspects of MCSs over central Europe. Our results indicate that MCSs are not rare in Poland as an annual mean of 77 MCSs and 49 days with MCS can be depicted for Poland. Their lifetime ranges typically from 3 to 6 h, with initiation time around the afternoon hours (1200–1400 UTC) and dissipation stage in the evening (1900–2000 UTC). The most frequent morphological type of MCSs is a broken line (58% of cases), then areal/cluster (25%), and then quasi-linear convective systems (QLCS; 17%), which are usually associated with a bow echo (72% of QLCS). QLCS are the feature with the longest life cycle. Among precipitation archetypes of linear MCSs, trailing stratiform (73%) and parallel stratiform (25%) are the most common. MCSs are usually observed from April to September, with a peak in mid-July. A majority of MCSs travels from the west, southwest, and south sectors. A total of 16 derecho events were identified (1.5% of all MCS and 9.1% of all QLCS); the majority of them were produced by a warm-season QLCS, whereas only 4 were produced by cold-season narrow cold-frontal rainbands. Warm-season derechos produced a bigger impact than did cold-season events, even though their damage paths were shorter.

## 1. Introduction

According to estimates based on lightning data and ground-based human observations of audible thunder (SYNOP reports), more than 150 days with thunderstorm occur each year in Poland, and for a specific location that number changes from 15 days over the northeastern part of the country up to 35 over the southeast (Bielec-Bąkowska 2003; Taszarek et al. 2015). Estimates provided by Taszarek et al. (2018) suggest that most of these storms develop in a weak shear regime (a median of 0–6 km AGL shear of 10–12 m s$^{-1}$) and consist mainly of isolated cells and weak multicell activity. Better-organized storm complexes that create their own internal circulation and usually require stronger environmental wind shear are called mesoscale convective systems (MCS; Markowski and Richardson 2010). They typically last from a few to several hours and contain continuous area of precipitation extending to a distance of 100 km or more (Houze 1993, 2004, 2019).

Although MCSs are common in Europe during summertime (Morel and Senesi 2002a,b), their morphological characteristics remain unknown because no quantitative and qualitative estimates with radar data

Denotes content that is immediately available upon publication as open access.

*Corresponding author*: Artur Surowiecki, artur.surowiecki@uw.edu.pl

DOI: 10.1175/MWR-D-19-0412.1

*Publisher's Note:* This article was revised on 27 October 2020 to include the CC BY reuse license that should have been applied when originally published.

had been performed. As opposed to satellite images, radar data allow for a more accurate detection of MCSs and their corresponding morphological features. Improvements in the quality and coverage of radar data along with prolonging measurement periods over the last year provide increasingly better possibilities for constructing climatologies of convective phenomena. However, the disadvantage of a radar-based approach is a more subjective identification and classification process (Jirak et al. 2003) that is affected by the varying quality of radar data (e.g., as a function of distance to the radar site). This issue may lead to the necessity of a manual identification of MCSs. In this context, satellite-based climatologies offer more spatially homogeneous results but provide less information about system morphology.

MCSs are responsible for a significant portion of warm-season rainfall in midlatitudes such as the central part of the United States (Fritsch et al. 1986; Ashley et al. 2003; Schumacher and Johnson 2006; Haberlie and Ashley 2019), eastern China (He et al. 2016), or Europe (Rigo and Llasat 2004, 2007; Punkka and Bister 2005, 2015). They are also capable of producing severe-weather phenomena like damaging winds (Johns and Hirt 1987; Ashley and Mote 2005; Cohen et al. 2007; Mathias et al. 2017; Taszarek et al. 2019), tornadoes (Trapp et al. 2005; Gallus et al. 2008), and flash floods (Bosart and Sanders 1981; Doswell et al. 1996, Schumacher and Johnson 2005, 2006; Peters and Schumacher 2014; Moore et al. 2012; Terti et al. 2017; Zhang et al. 2019). MCSs occur in a broad variety of forms and can be classified in several ways. The most commonly used classification is based on their morphological features (Bluestein and Jain 1985; Blanchard 1990) and the relationship between propagation of the system and position of the precipitation area (Parker and Johnson 2000). The majority of studies consider linear modes of MCSs because they have the highest potential for producing severe weather. However, selected elaborations considered also nonlinear types, which usually remain stationary and are capable of producing heavy rainfall (Gallus et al. 2008; Zheng et al. 2013).

Radar-based MCS climatologies were constructed mainly for the central and eastern parts of the United States where during spring and summer they produce a big impact on society and infrastructure (Geerts 1998; Parker and Johnson 2000; Fritsch and Forbes 2001; Jirak et al. 2003). Burke and Schultz (2004) and Celiński-Mysław et al. (2020) studied also cold-season bow echoes developing from different convective modes. In some approaches, automated algorithms were used to detect MCSs (Fiolleau and Roca 2013; Haberlie and Ashley 2018a,b, 2019). Selected studies focused also on mesoscale convective complexes (Maddox 1980; Augustine and Howard 1988), persistent elongated convective systems (Anderson and Arritt 1998) and quasi-linear convective systems (QLCS) including derechos—a particularly dangerous system producing a widespread wind damage (Bentley and Mote 1998; Bentley and Sparks 2003; Guastini and Bosart 2016; Celiński-Mysław and Matuszko 2014; Gatzen et al. 2020). Derechos are not always associated with systems meeting the criteria for MCS because cold-season cases are frequently related to narrow cold-frontal rainbands (NCFR; Hobbs and Biswas 1979; Koch and Kocin 1991; Gatzen 2011).

In addition to research conducted for the area of the United States, MCS climatologies in midlatitudes were also constructed for subtropical parts of South America (Velasco and Fritsch 1987; Salio et al. 2007) and China (Yang et al. 2015). Only a few studies were carried out for Europe. However, most of them were based on infrared satellite imagery (Morel and Senesi 2002a,b; Lewis and Gray 2010; Kolios and Feidas 2010) and did not provide insight about morphological archetypes of MCSs. Among radar-based approaches Rigo and Llasat (2004, 2007) focused on MCSs that produce heavy rain over Spain. Punkka and Bister (2005, 2015) studied intense and nonintense MCSs and their associated environments over an 8-yr period in Finland. However, none of the prior studies over Europe provided climatological aspects of morphological archetypes of MCSs. Studies about MCS occurrence in Poland are uncommon. Prior research concerned mainly high-impact case studies (Walczakiewicz and Ostrowski 2010; Widawski and Pilorz 2018; Taszarek et al. 2019; Poręba and Ustrnul 2020). A few collaborations focused on the occurrence of bow echos and derechos over the last few years (Celiński-Mysław and Matuszko 2014; Celiński-Mysław and Palarz 2017; Celiński-Mysław et al. 2019, 2020).

The main goal of this analysis is to take advantage of 10 years of continuous radar observations in Poland to construct a comprehensive climatology of MCSs. Our study is one of the first attempts for a European country to determine radar-based qualitative and quantitative assessments of certain MCSs archetypes over such a long period. In addition, we also provide a separate section devoted to climatological aspects of derechos over the same period because their occurrence in Europe is becoming an increasingly important topic over the last few years. These types of storms frequently produce considerable damage to infrastructure and immense societal impacts, which makes their return periods important to evaluate. Nowadays, more accessible remote sensing data and a constantly increasing number of severe-weather reports allow one to identify derechos in the way that was not possible 20–30 years ago (Hamid 2012; Celiński-Mysław and Matuszko 2014; Toll et al.

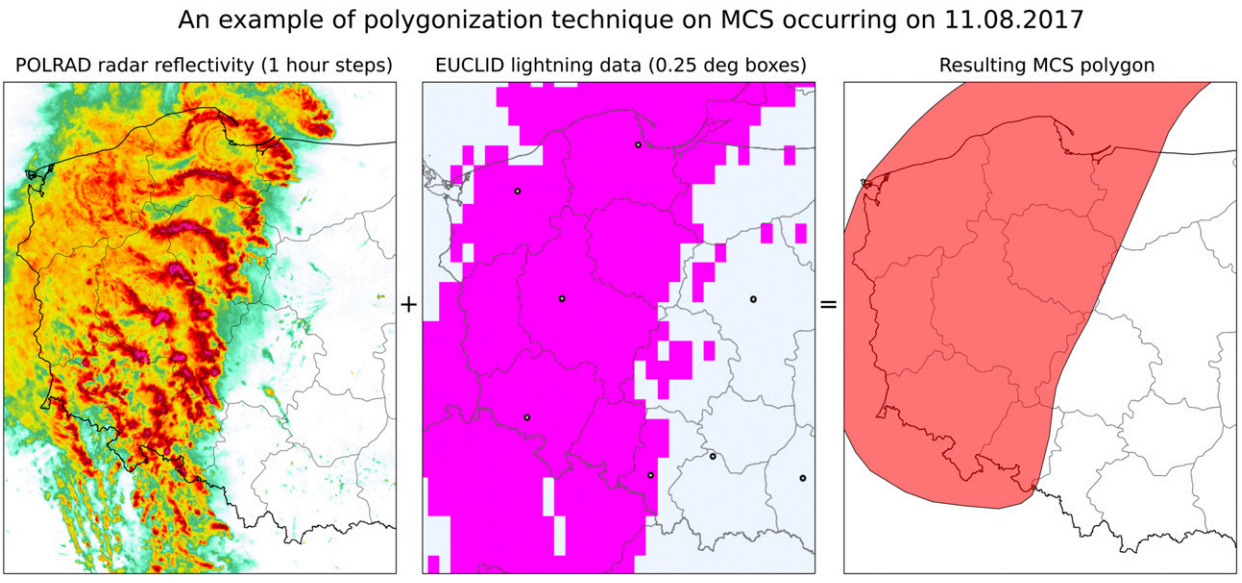


FIG. 1. An example of the polygonization technique (applied on MCS from 11 Aug 2017) used in the study.

2015; Gospodinov et al. 2015; Taszarek et al. 2019; Gatzen et al. 2020; Mathias et al. 2019).

## 2. Dataset and method

### *a. MCS definition and identification technique*

The MCS definition proposed by Houze (1993) refers to the size of the entire system. According to that definition, MCS is a cloud system that consists of lightning activity and a continuous precipitation area of 100 km or more in at least one direction. For the purposes of this study, we use a more precise definition that is based on work by Parker and Johnson (2000) and consider MCS when the following criteria are fulfilled:

1) the system develops as a result of a deep moist convection (Doswell et al. 1996),
2) the system contains a convective precipitation zone with radar reflectivity of at least 40 dB$Z$ and presence of lightning activity,
3) the entire system (including also a contiguous stratiform precipitation zone attached to convective cores) extends to a distance of at least 100 km, and
4) the above criteria are fulfilled during a time frame of at least 3 h.

We also mention that spatial or temporal criteria used for MCS identification are specific to the type of source data (radar or satellite) being used in that process (Geerts 1998). In addition to Parker and Johnson (2000) our radar-based definition of MCS is also comparable to that from studies by Geerts (1998), Coniglio et al. (2010), and Pinto et al. (2015).

Identification of MCSs was performed manually by taking into account radar and lightning data in the 10-min intervals over the period of 2008–17. The identification process contained a few steps. First, we thoroughly examined radar data (maximum reflectivity product) to detect all larger convective structures that could possibly meet MCS criteria. Then, we cross-referenced each case with lightning data. In the next step, we derived time intervals (start and end time) of each case that met MCS criteria. Last, polygons indicating spatial and temporal extent of each MCS case were created given start and end time. An example of this procedure is presented in Fig. 1. An attempt to create an automated algorithm for detecting spatial extent of MCSs was made, but it was unfortunately burdened with errors associated with the varying quality of radar data in both the spatial and temporal aspects. The algorithm was unable to distinguish between more than one MCS merging together and had a bias associated with distance to the radar, which means that, given a specific reflectivity threshold, it had a tendency to detect more MCSs close to the radar site. Although algorithms helped to preliminarily identify some of the MCS cases in the first step of the analysis, a thorough manual investigation of each case was necessary to provide more accurate estimates and assign morphological (as in Fig. 2), and precipitation (as in Fig. 3) archetypes (further details are available in section 2b). In total, 766 MCSs were identified over a period of 2008–17, each containing information about spatial extent, start and end time (in UTC), and corresponding morphological features. In the final step, the R programing language

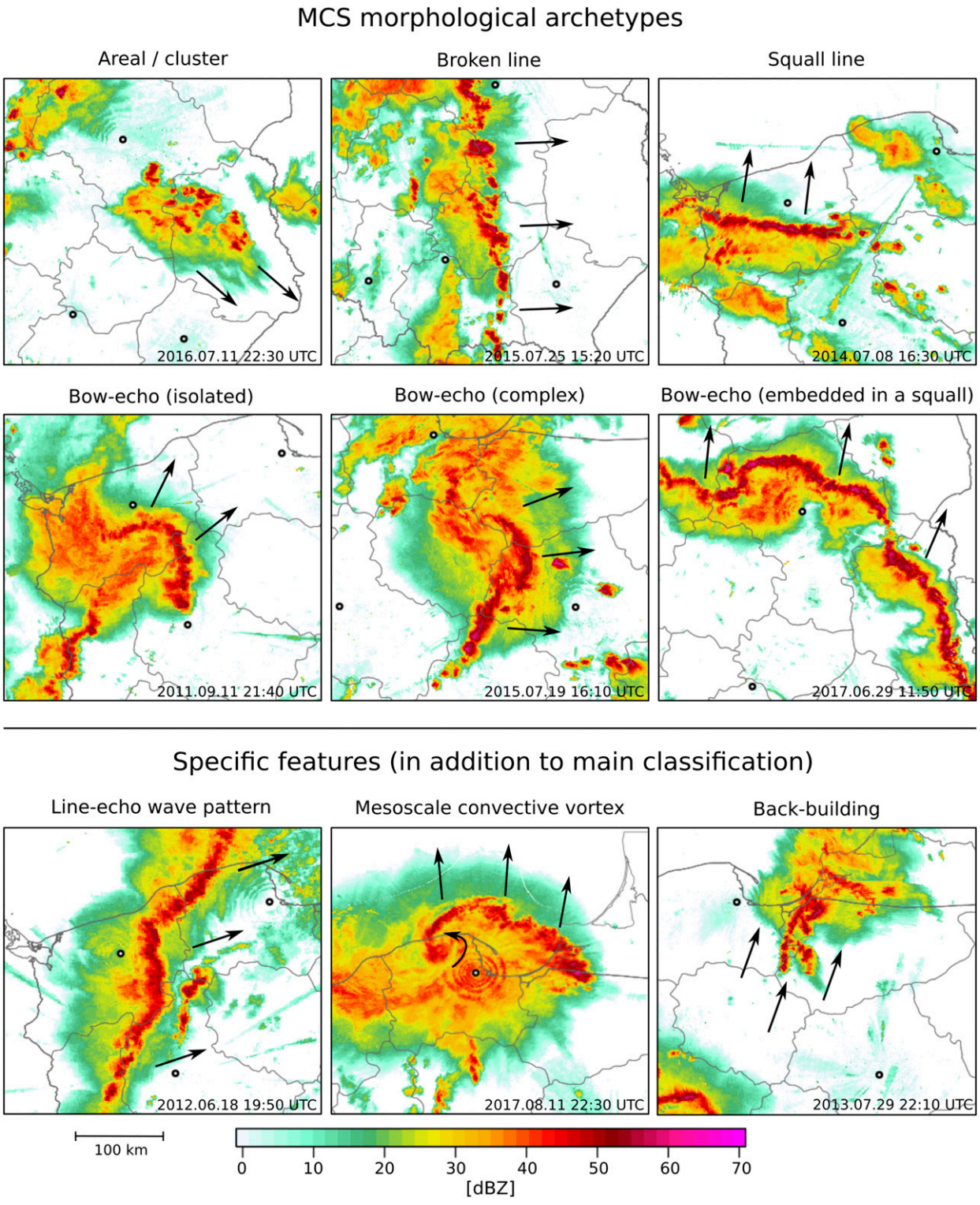


FIG. 2. MCS morphological archetypes used in this study (see Table 1 and section 2b). Open circles indicate locations of radar sites.

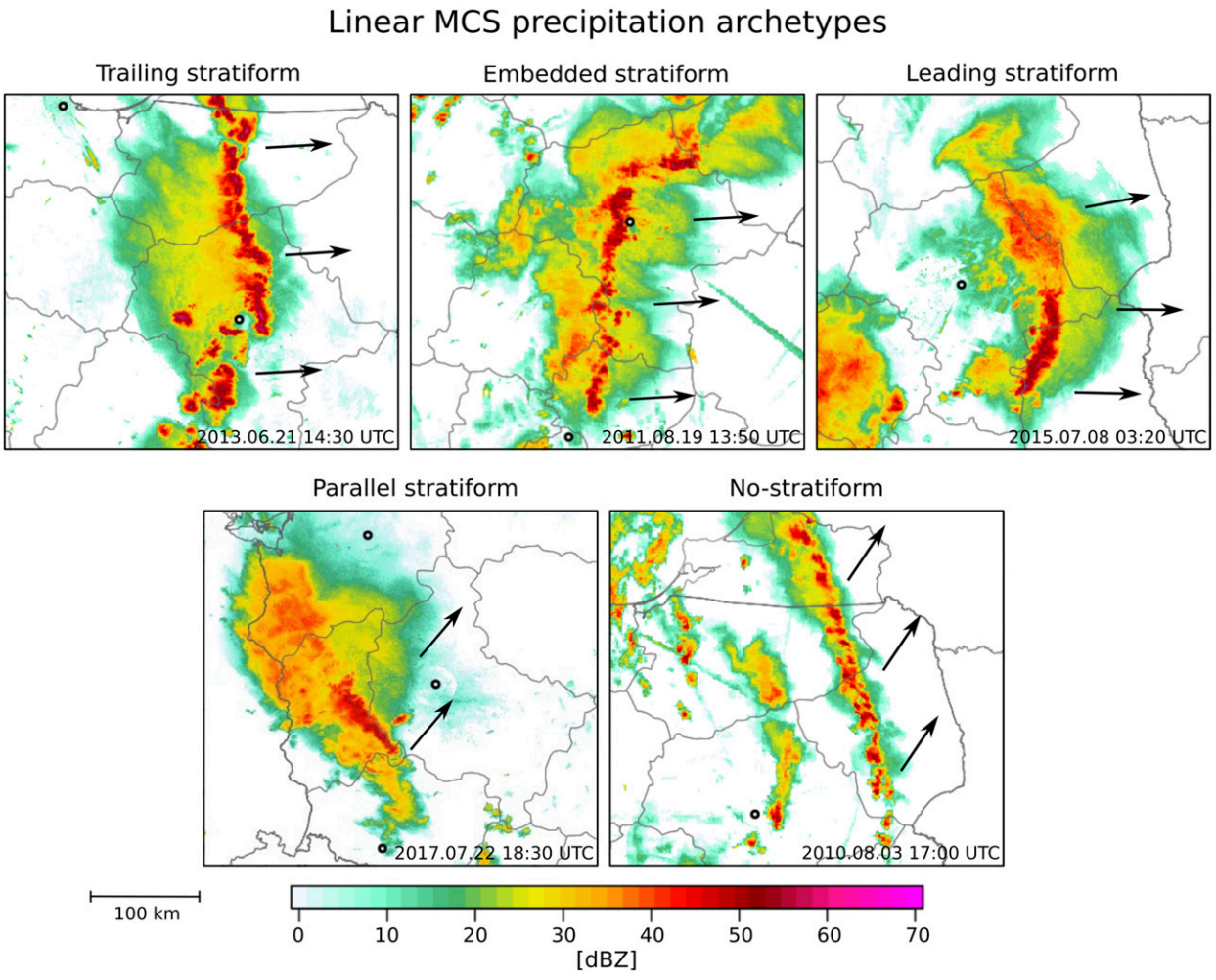


FIG. 3. MCS precipitation archetypes used in this study (see Table 2 and section 2b). Open circles indicate locations of radar sites.

(R Core Team 2013) was used to construct spatial and temporal statistics.

### b. *Morphological and precipitation MCS archetypes*

To discriminate between MCS morphological archetypes, we used a modified classification initially proposed by Bluestein and Jain (1985). In this study, we distinguish three main categories: a disorganized complex of convective cells (areal/cluster), a broken line of convective cells (broken line), and QLCS with and without bow echo (squall/bow echo; Fig. 2). Categorization of bow-echo events as isolated, complex, or embedded was based on Klimowski et al. (2004). A similar method in MCS research was also applied by Blanchard (1990) and Loehrer and Johnson (1995). Additional features of MCSs (in addition to main classification) such as line-echo-wave-pattern (LEWP; Nolen 1959), mesoscale-convective-vortex (MCV; Bartels and Maddox 1991) and back-building (Schumacher and Johnson 2005, 2006, 2008, 2009) types are also presented in Fig. 2. These were detected as an addition to analysis of radar data and are presented here as an example of such features accompanying MCS occurrence in Poland.

Classification of MCS precipitation archetypes was derived from Parker and Johnson (2000) and included trailing stratiform, leading stratiform, and parallel stratiform modes (Fig. 3). In addition to this categorization, we also added "embedded in stratiform (ES)" and "no stratiform" following Gallus et al. (2008) and Zheng et al. (2013). In our study, more than one precipitation type could have been assigned to a single MCS, as was often a case for long-lived systems.

### c. *Radar data*

The radar network in Poland (POLRAD; Jurczyk et al. 2008) is maintained by the Polish Institute of Meteorology and Water Management (IMGW-PIB)

TABLE 1. Mean annual number and fraction of certain MCS types, on the basis of 766 MCS cases from 2008 to 2017.

| MCS type | Mean per year | Fraction |
|---|---|---|
| Areal/cluster | 19.1 | 24.9% (among all MCS) |
| Broken line | 44.3 | 57.9% (among all MCS) |
| Quasi-linear convective system | 13.2 | 17.2% (among all MCS) |
| Squall line | 3.6 | 27.3% (among all QLCS) |
| Bow echo (isolated) | 2.2 | 16.7% (among all QLCS) |
| Bow echo (complex) | 2.3 | 17.4% (among all QLCS) |
| Bow echo (squall line embedded) | 5.1 | 38.6% (among all QLCS) |
| Specific features (in addition to main classification) | | |
| Mesoscale convective vortex | 2.7 | 3.5% (among all MCS) |
| Back building | 2.8 | 3.7% (among all MCS) |
| Line-echo wave pattern | 1.1 | 8.3% (among all QLCS) |
| Derecho | 1.2 | 9.1% (among all QLCS) |

and began operational work in the early 2000s. The network consists of eight C-band Doppler radars: Meteor 500C (Poznań, Brzuchania, Świdwin), Meteor 1500C (Legionowo, Gdańsk), and dual-polarimetric Meteor 1600C (Pastewnik, Rzeszów, Ramża) of Selex SI Gematronik (the locations of the radars are presented in the figures in the latter part of the paper). Further details on the POLRAD network are available in Ośródka et al. (2014). Data provided for the purposes of this study had a temporal step of 10 min and a spatial resolution of 1 km, which allowed for identification of even local convective features. Only a "CMAX" product (maximum reflectivity in a vertical column) was used in this study.

Radar data face a number of disadvantages that affect their quality. The most important is the decreasing strength of the radar signal with distance from the radar. This produces bias in measured reflectivity, which is on average higher several kilometers from the radar as compared with distances of more than 100 km (Chumchean et al. 2004). In specific situations this may affect reflectivity and spatial extent criteria assigned for the definition of MCS in this study. Because of this limitation, identification efficiency of MCSs occurring on the peripheries of the POLRAD network (especially over northeastern and eastern Poland) may be lower than for other parts of the country. Some MCSs may have been omitted during the identification process when convective structures moved outside POLRAD network range to neighboring countries. Our MCS database may also be slightly affected by problems such as temporal breakdowns of selected radars, service periods, and changes in settings (e.g., the Ramża radar in 2008 had a tendency to overestimate reflectivity relative to other radars). Another minor disadvantage is that radar data are burdened with erroneous radar scannings resulting from signal distortions (e.g., Wi-Fi networks) that implicate enhanced dB$Z$ values, but that issue did not play a major role in MCS identification process.

### d. *Lightning data*

European Cooperation for Lightning Detection (EUCLID; Poelman et al. 2016; Schulz et al. 2016) lightning data with a spatial resolution of 0.25° and 1-h step were used in the analysis as supporting information to fulfill the MCS definition (see section 2a). If no lightning activity was recorded, then MCS could not be confirmed. EUCLID contains 149 sensors located throughout Europe and has a spatial detection accuracy within a range of 100–500 m, with a detection efficiency of cloud-to-ground lightning of more than 90% (Schulz et al. 2016). In the investigated period (2008–17), the number of sensors in the network slightly increased, but even though stroke detection efficiency has improved, the flash detection efficiency remained stable through these years (Schulz et al. 2016). Because in this study we use only flash data, these changes should not produce temporal bias and influence our results in a significant way. Although the hourly step of EUCLID data differs from the 10-min intervals of radar scans, this issue had almost no influence on MCS identification. For the area of Poland, the total number of detected cloud-to-ground lightning was 5 378 826. That number varied in individual years from 415 250 to 738 723.

### e. *Definition of a derecho*

We adopted a derecho definition proposed by Johns and Hirt (1987), which was used in several prior studies (e.g., Evans and Doswell 2001; Coniglio et al. 2004; Gatzen 2011; Celiński-Mysław and Matuszko 2014). To fulfill requirements for a derecho, we used severe wind data from SYNOP reports and the European Severe Weather Database (ESWD; Dotzek et al. 2009) containing information about peak intensity and inflicted damage [using the "TORRO" (Meaden 1976) and Fujita (Fujita 1971) scales]. Radar data were used as supporting information to identify propagation direction and

TABLE 2. Precipitation types among broken lines and QLCS (more than one type can apply per MCS), on the basis of 766 MCS cases from 2008 to 2017.

| MCS precipitation feature | Mean per year | Fraction |
|---|---|---|
| Trailing stratiform | 41.9 | 72.9% (among broken lines and QLCS) |
| Embedded stratiform | 9.6 | 16.7% (among broken lines and QLCS) |
| Leading stratiform | 6.2 | 10.8% (among broken lines and QLCS) |
| Parallel stratiform | 14.4 | 25.0% (among broken lines and QLCS) |
| No stratiform | 9.6 | 16.7% (among broken lines and QLCS) |

spatial extent of derechos moving through territory of Poland. We determined the length of derecho track using the first and last severe wind report in the damage swath produced by a parent convective system (area consisting of chronologically arranged and continuous group of severe wind reports). Similar to the classification proposed by Coniglio et al. (2004), we rated derechos with low-, moderate-, and high-intensity categories. However, unlike Coniglio et al. (2004), we categorized low-end derechos as not exceeding the F1/T2 category within wind reports. For high-intensity events, wind damage exceeded F1/T2 category and derecho was associated with a significant impact to infrastructure and society (which had been rated subjectively). All detected derecho events were divided into two groups [as in Gatzen et al. (2020)] for warm-season derechos (occurring from April to September) and cold-season derechos (occurring from October to March). Cold-season derechos in Poland were mostly produced by convective systems that did not meet the MCS criteria used in this study. However, to obtain estimates consistent with Gatzen et al. (2020), we decided to consider non-MCS derecho events occurring in a form of NCFRs (Gatzen 2011). Gatzen et al. (2020) suggested that derecho-producing NCFRs develop usually on a fast-moving cold front in an environment with a low convective available potential energy (CAPE) and high vertical wind shear supported by a strong synoptic-scale ascent. These MCS-like systems have a strongly elongated shape and a very narrow linear zone of locally enhanced reflectivity with weak lightning activity. Unlike MCSs, these formations do not contain areas with reflectivity exceeding 40 dB$Z$ that persist over a long time.

### *f. Potential limitations*

The biggest limitations in this study involve the radar data. Distant convective objects may be attenuated by strong convective cores occurring closer to the radar. Second, since MCS must last at least 3 h and extend over an area of at least 100 km, fast-moving systems and especially those occurring on the edges of the POLRAD network range could not be identified. Therefore, our database is biased toward the central part of the domain where a higher number of detections were possible relative to the edges, and especially northeastern Poland (lack of radar in that part of country). Moreover, as a result of MCS moving predominantly from southwestern and southern because they left the research domain before reaching a temporal MCS criteria of 3 h. Conversely, fading MCSs entering southwestern or southern Poland could also not reach 3-h criteria. It is also possible that, because of manual and subjective analysis of all cases, some minor human-factor inhomogeneities may be incorporated in the database.

To display annual and diurnal variability of MCSs we also use a technique of moving windows aimed at removing noise resulting from the limited sample size. As a result, some details may be smoothed out but readability of the results improves. The magnitude of smoothing is a compromise between available sample size and representativeness of the results.

## 3. Results

### *a. Frequency of a certain morphological and precipitation MCS archetypes*

In total 766 MCSs occurring over 488 days were identified over the period 2008–17, giving an annual mean of 77 MCSs and 49 days with MCS. Among morphological types, a broken line turned out to be the most frequent (58% of all MCSs in the database, with a mean of 44 per year; Table 1 and Fig. 2). The second was areal/cluster type consisting of 25% of all

TABLE 3. Number of MCS and MCS days in analyzed years, on the basis of 766 MCS cases from 2008 to 2017.

| Year | 2008 | 2009 | 2010 | 2011 | 2012 | 2013 | 2014 | 2015 | 2016 | 2017 |
|---|---|---|---|---|---|---|---|---|---|---|
| MCS | 66 | 93 | 70 | 77 | 85 | 70 | 74 | 62 | 84 | 85 |
| MCS days | 46 | 55 | 45 | 57 | 52 | 47 | 50 | 44 | 43 | 49 |
| MCS/(MCS day) ratio | 1.4 | 1.7 | 1.6 | 1.4 | 1.6 | 1.5 | 1.5 | 1.4 | 2.0 | 1.7 |

TABLE 4. Mean annual number of MCS and MCS days in analyzed months, on the basis of 766 MCS cases from 2008 to 2017.

| Month | Mar | Apr | May | Jun | Jul | Aug | Sep | Oct | Nov | Year |
|---|---|---|---|---|---|---|---|---|---|---|
| Mean of MCS (per year) | 0.4 | 1.6 | 12.5 | 17.4 | 26.4 | 14.7 | 2.9 | 0.6 | 0.1 | 76.6 |
| Mean of MCS days (per year) | 0.3 | 1.4 | 9.1 | 11.4 | 13.6 | 10.4 | 2.9 | 0.6 | 0.1 | 48.8 |
| MCS/(MCS day) ratio | 1.3 | 1.1 | 1.4 | 1.5 | 1.9 | 1.4 | 1 | 1 | 1 | 1.6 |

cases and providing a mean of 19 per year. The least frequent was squall/bow echo (we also use QLCS term as an alternative for this category) with a share of 17% (13 cases per year). Among QLCS as much as 72% (10 cases per year) were associated with the presence of a bow echo in various modes (''squall line embedded'' being the most frequent; Table 1 and Fig. 2). Among specific features of MCSs that were classified in addition to main classification, LEWP was identified in 11 MCSs (8.3% among all QLCS), MCV in 27 (3.5% among all MCSs), and back building in 28 (3.7% among all MCSs). Back-building MCSs are typically rare but are often associated with heavy precipitation and flash-flooding situations (e.g., 29 July 2013 and 16 May 2014; Siwek 2016). A comparison of back-building systems with ESWD reports yielded that in 64% of cases a heavy rain event was reported inside the MCS polygon. Derecho category was reached in 9.1% of all QLCS (discussed in details in a further part of the paper).

Precipitation archetypes considered within broken lines and squall/bow echo (Fig. 3) yielded that trailing stratiform precipitation occurred in 73% of cases (42 per year; Table 2). The second most prevalent archetype turned out to be a parallel stratiform (14.4 cases per year with a share of 25%). Embedded, leading, and no-stratiform types were less frequent and occurred in approximately every fifth to seventh linear MCS (6–10 per year).

### b. *Year-to-year, annual, and diurnal variability*

MCSs in Poland demonstrate a strong year-to-year variability. In 2009, 2012, 2016, and 2017 more than 83 cases were reported, with a record of 93 in 2009 (Table 3). The lowest frequency took place in 2008 and 2015 (66 and 62 cases, respectively). Variability of days with MCS was lower and ranged from 43 and 44 (2016 and 2015) to as much as 55 and 57 (2009 and 2011). Interannual changes in the mean ratio of MCS cases to days with at least one MCS are small and vary from 1.4 to as much as 2.0, with a 10-yr mean of 1.6 (Tables 3 and 4).

Investigation of annual cycle indicates that MCSs usually start to occur in early March (a mean of 0.4 cases per year; Table 4) and that the last ones are recorded as late as November (only one case in the entire database). During winter, no MCSs were identified over the territory of Poland during the analyzed time frame. In May, the mean annual number of MCSs rapidly increases to 12 cases per year (Fig. 4, Table 4). This growth slows in June (18 per year) and then accelerates again to reach peak in mid-July (26 per year with an average of almost 2 MCSs per day with MCS). After that point, activity rapidly drops to 15 cases per year in August and 3 in September. The annual cycle in the division for specific MCS morphological archetypes indicates that most of the systems from March to May are areal/clusters and broken lines (Fig. 4). The squall/bow-echo category has a delayed annual cycle and its frequency starts to rapidly increase in June and lasts until August. Note that in mid-June there is a small decrease in the occurrence of broken lines and a slowdown in areal/cluster MCSs.

Typically, MCSs in Poland last from 3 to 6 h. However, duration strongly depends on the specific MCS archetype,

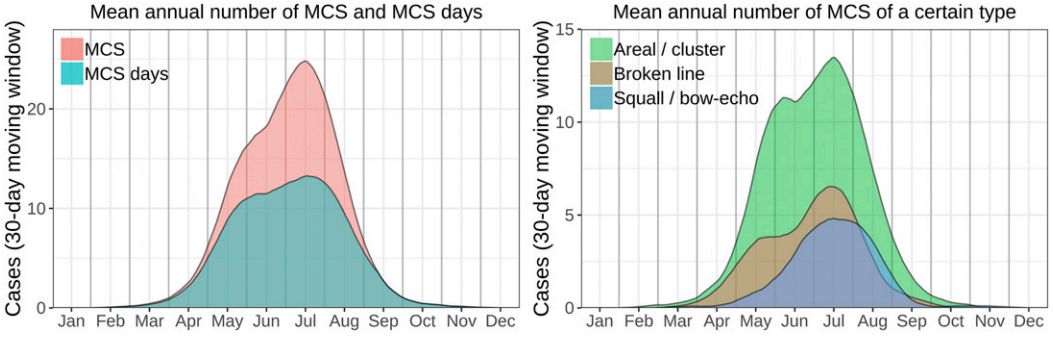


FIG. 4. Mean annual number of MCS and MCS days computed with a 30-day moving window, based on 766 MCS cases in Poland from 2008 to 2017. Note that month labels indicate the 15th day of each month.

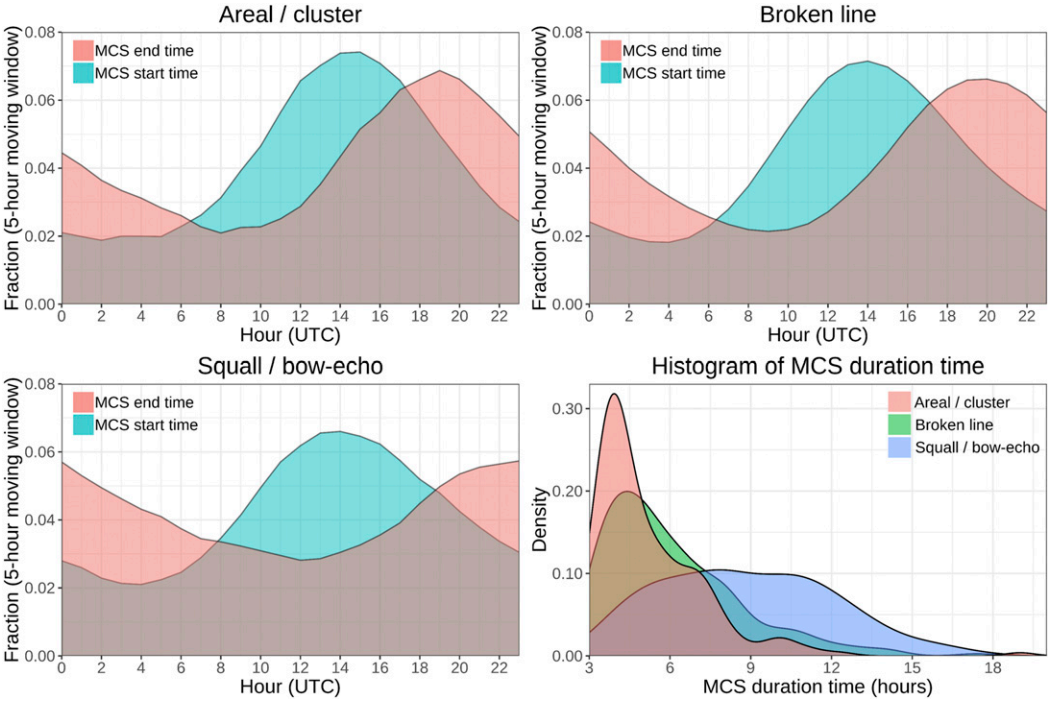


FIG. 5. Mean hour of MCS start and end time and (bottom right) histogram for certain MCS types, on the basis of 766 MCS cases in Poland from 2008 to 2017. Start and end time charts are computed with a 5-h moving window.

with areal/clusters having the shortest lifetime of 4–5 h and squall/bow echo having the predominant duration of 8–10 h (Fig. 5). Some cases of areal/clusters and broken lines can last as long 15 h, whereas squall lines and bow echos reach even 19 h. However, this estimate is strongly influenced by our domain size, as MCSs moving off the radar range can no longer be tracked. The majority of MCSs start usually in the early afternoon hours (1200–1400 UTC) and fade around 1900–2000 UTC, with the exception of squall/bow echos having their most frequent end time at midnight (Fig. 5). This is consistent with a typical diurnal cycle of lightning activity over

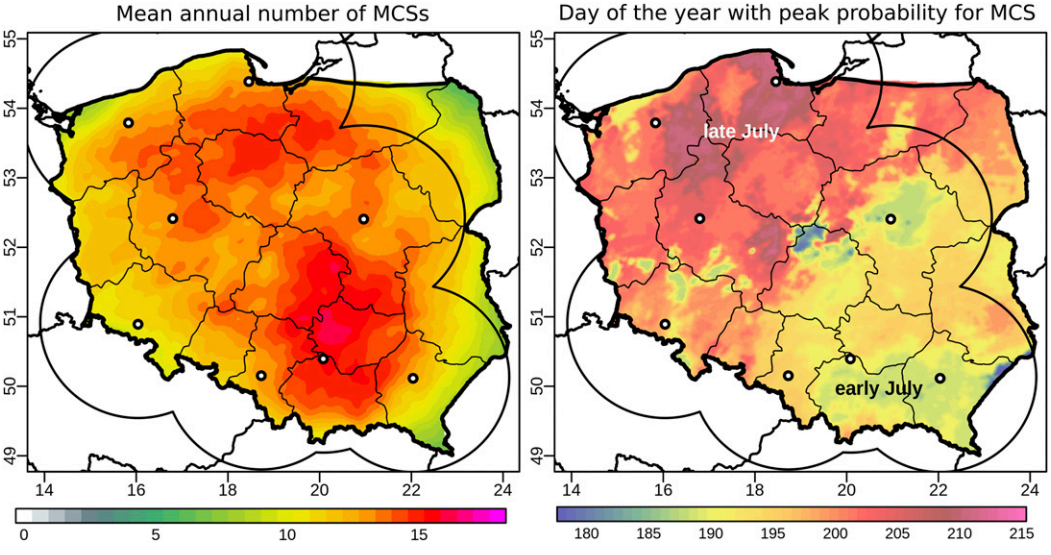


FIG. 6. (left) Mean annual number of MCSs and (right) day of the year with peak probability for MCS estimated with a 30-day moving window, based on 766 MCS cases in Poland from 2008 to 2017. Open circles indicate locations of radar sites and 160-km buffer zones.

Poland and with systems producing higher flash counts that usually last longer (Taszarek et al. 2015).

### c. Spatial variability

Annual mean number of MCSs over a specific location ranges generally from 10 to 17, with peak values observed over south-central Poland (Fig. 6). However, as discussed in section 2c, density values obtained over edges of the domain, especially southeastern and northeastern Poland, may be burdened with underestimation, and thus caution should be taken when interpreting these results. Despite the aforementioned bias, an interesting spatial pattern in MCS occurrence is observed over specific months. In early summer (June and July), most of the MCSs are reported over the eastern and southeastern part of the country (4–6 per month for the specific location), whereas in August and September peak activity shifts to northwestern Poland (Fig. 7). That kind of temporal shift is also present in the estimation of the day of the year, with the highest frequency of MCSs (as a function of a 30-day moving window) presented in Fig. 6b. Peak probability for MCS over southeastern Poland is estimated in early July, whereas over northwestern Poland it is delayed to late July and early August.

Year-to-year changes in the spatial patterns for MCS demonstrate their considerable variability (Fig. 7). The annual number of MCSs for a specific location varies from only a few cases (e.g., northwestern Poland in 2008) to as many as 27 (south-central Poland in 2017). During years with low activity, the maximum annual number of MCS did not exceed 15–17 (2010, 2014, and 2015). In most of the years, the lowest number of MCSs for a specific location was around 5–10. Local maxima in MCS activity feature also with high variability. For example, in 2009, 2012, and 2014 activity concentrated mostly over western Poland, whereas in 2015, 2016, and 2017 the maximum was over the southeast (Fig. 8).

Investigation of spatial variability in fraction of certain MCS morphological archetypes (Fig. 9) revealed that areal/clusters have the biggest share over southeastern Poland (30%–40%). From the climatological point of view, this area features the lowest vertical wind shear and highest CAPE relative to the remaining part of the country (Taszarek et al. 2018), which may support slow-moving poorly organized systems. Conversely, broken lines have the highest fraction over northwestern Poland (55%–65%), which is under the strong influence of the Baltic Sea and has the lowest CAPE and highest shear relative to the rest of Poland. Such distribution may be explained by the fact that higher vertical wind shear promotes better organization of the cold pools that promote linear systems (Rotunno et al. 1988; Weisman and Rotunno 2004) and that there is a higher frequency of cold fronts over northwestern Poland (also supporting broken lines). The squall/bow-echo category has a less defined spatial peak, but an enhanced fraction of around 40% occurs over southwestern Poland. This is likely to be associated with large MCSs entering Poland from Germany and the Czech Republic in the late-afternoon hours (Taszarek et al. 2015).

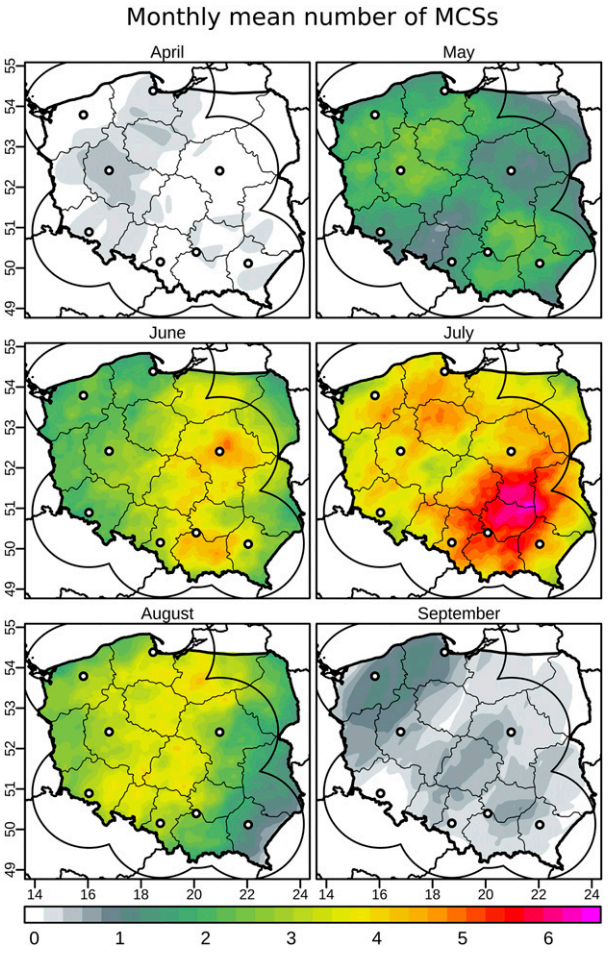


FIG. 7. Monthly mean number of MCS (with a 5 km × 5 km focal mean smoothing), on the basis of 766 MCS cases in Poland from 2008 to 2017. Open circles indicate locations of radar sites and 160-km buffer zones.

### d. Variability in MCS movement

The most common propagation of MCSs in Poland is associated with movement direction from the west and west-southwest (Fig. 10). Depending on the region of Poland, the total percentage of MCSs that moves from these directions reaches 35%–40%. A considerable part (25%–40%) of the MCSs are also moving from the south, southwest, and south-southwest. There is a relatively small percentage of MCSs moving from the south

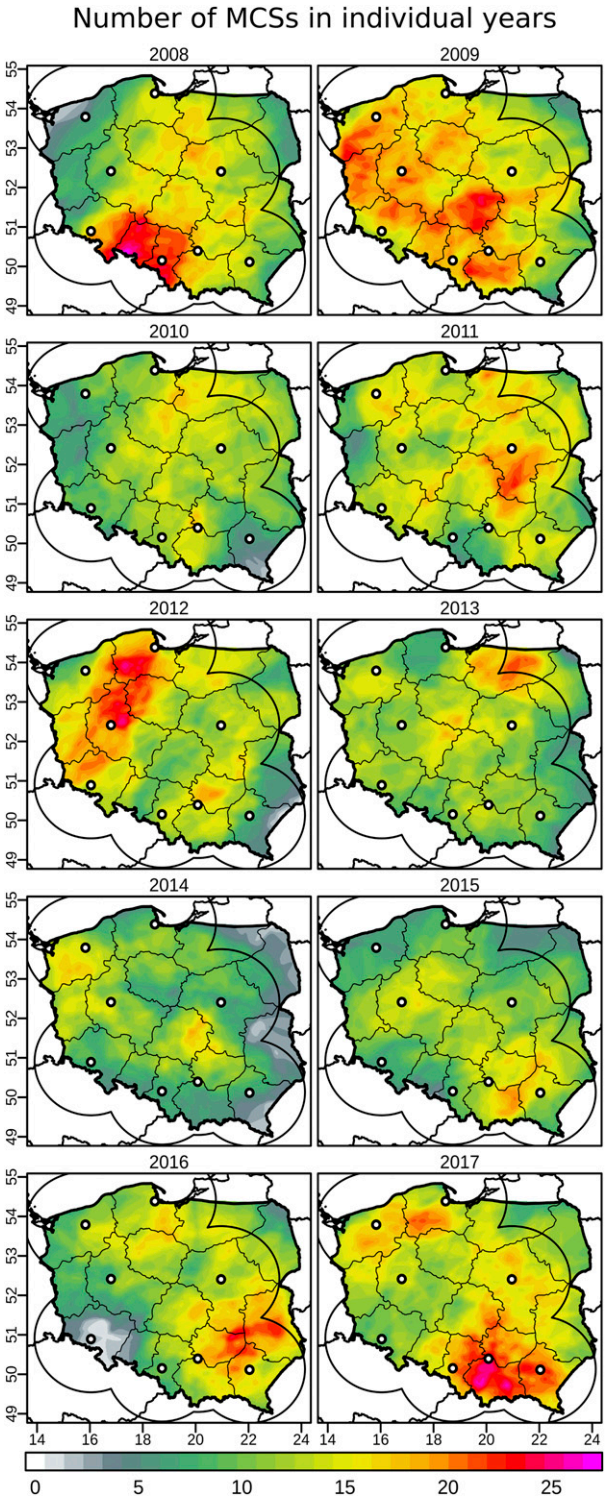


FIG. 8. Number of MCS in individual years (with a 5 km × 5 km focal mean smoothing), on the basis of 766 MCS cases in Poland from 2008 to 2017. Open circles indicate locations of radar sites and 160-km buffer zones.

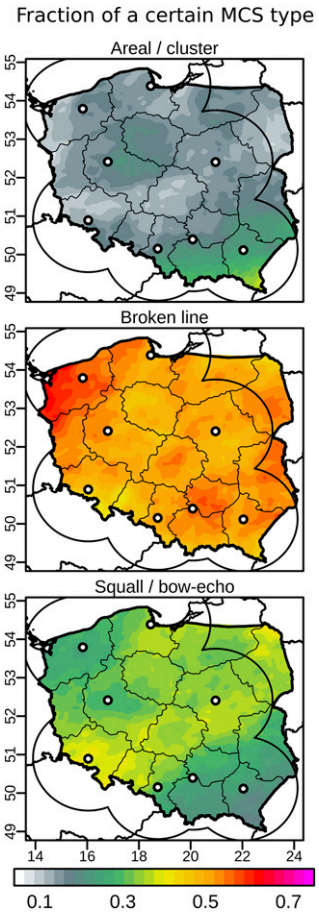


FIG. 9. Fraction of a certain MCS type (with a 5 km × 5 km focal mean smoothing), on the basis of 766 MCS cases in Poland from 2008 to 2017. Open circles indicate locations of radar sites and 160-km buffer zones.

in southeastern Poland when compared with the rest of the country. A very small share of MCSs (5%–15%) come from the east, southeast, and northwest directions or remain stationary (Fig. 10).

The direction of MCS movement is also slightly dependent on the particular morphological type of the system (Fig. 10). The most common sector for areal/cluster MCSs is a range from west to southwest and also south and south-southwest but with lower share. Broken lines share similar directions with areal/clusters, but their most frequent sector is west. QLCS have the biggest fraction in the west and west-southwest, with lower values reported for southwest, south-southwest, and south. Although selected cases were reported with the east-northeast, east, and east-southeast, it is very unlikely to have a squall line or a bow echo in Poland moving from eastern directions and ultimately any MCS moving from the north. This is consistent with synoptic circulation patterns supporting development

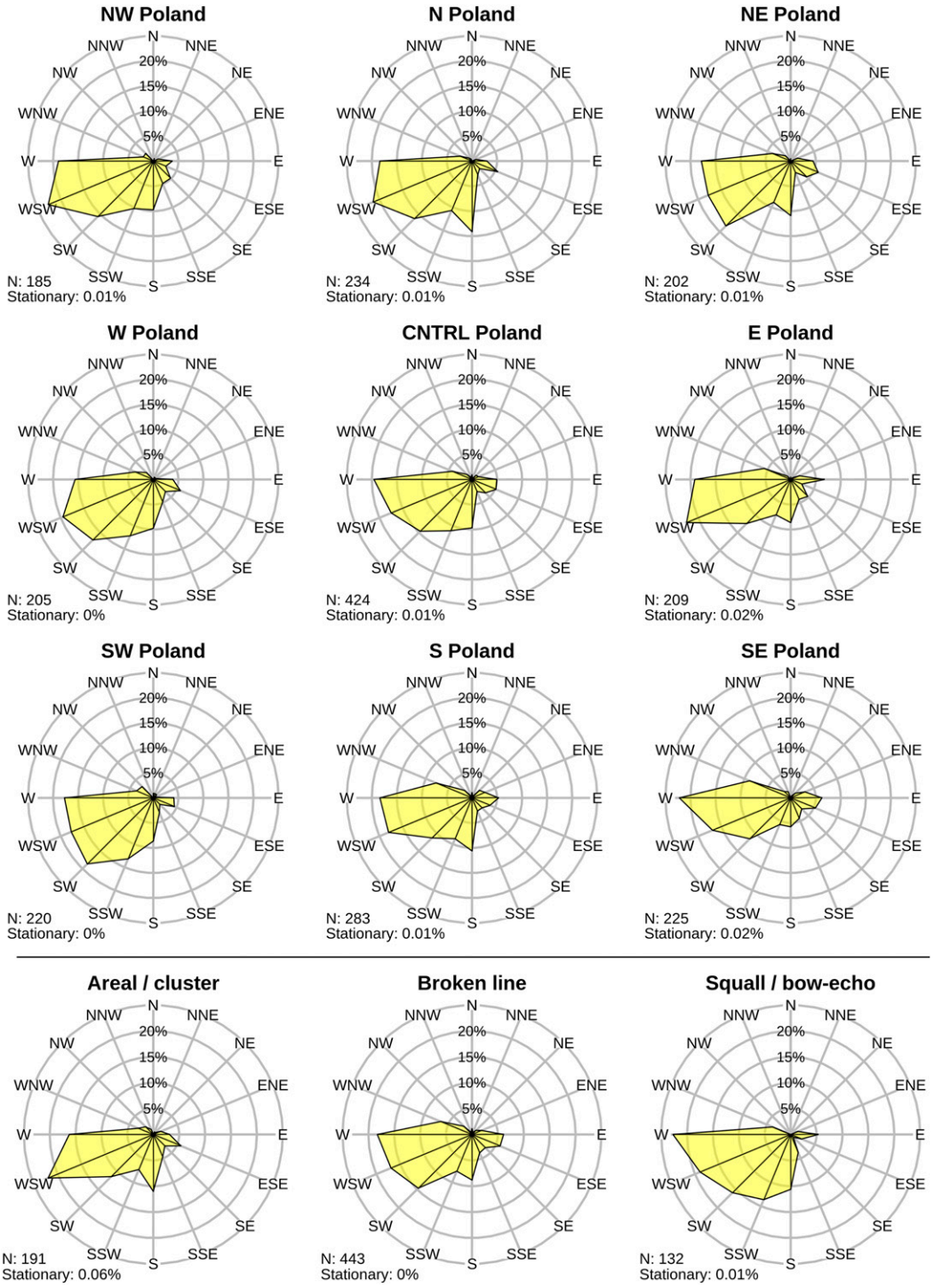


FIG. 10. Wind roses of MCS direction movement for different parts of Poland (note that the same MCS can be classified in more than one category) and (bottom) by certain archetypes, on the basis of 766 MCS cases in Poland from 2008 to 2017.

TABLE 5. List of derecho cases moving through the territory of Poland in years 2008–17.

| No. | Date | Peak damage rating[a] | Peak measured wind gust[b] | Total damage length[c] | No. of injured[b] | No. of killed[b] | Intensity[b] | Type |
|---|---|---|---|---|---|---|---|---|
| 1 | 26/27 Jan 2008 | F1/T2 | 33.8 m s$^{-1}$ | 1040 km | 0 | 0 | Moderate | NCFR |
| 2 | 22/23 Feb 2008 | F1/T2 | 31.0 m s$^{-1}$ | 1030 km | 0 | 0 | Moderate | NCFR |
| 3 | 1 Mar 2008 | F0/T1 | 31.0 m s$^{-1}$ | 1470 km | 0 | 0 | Low | MCS |
| 4 | 25 Jun 2008 | F0/T1 | 31.0 m s$^{-1}$ | 590 km | 0 | 0 | Low | MCS |
| 5 | 23 Jul 2009 | F2/T4 | 36.0 m s$^{-1}$ | 600 km | 44 | 7 | High | MCS |
| 6 | 20 Jul 2011 | F1/T3 | 29.0 m s$^{-1}$ | 820 km | 1 | 1 | Moderate | MCS |
| 7 | 6/7 Aug 2012 | F1/T3 | 44.5 m s$^{-1}$ | 560 km | 0 | 0 | High | MCS |
| 8 | 29 Jul 2013 | F1/T3 | — | 660 km | 0 | 0 | Moderate | MCS |
| 9 | 9 Jan 2015 | F0/T1 | 28.0 m s$^{-1}$ | 785 km | 0 | 0 | Low | NCFR |
| 10 | 7/8 Jul 2015 | F1/T2 | 34.0 m s$^{-1}$ | 650 km | 2 | 1 | Moderate | MCS |
| 11 | 19 Jul 2015 | F1/T3 | 29.0 m s$^{-1}$ | 825 km | 8 | 1 | High | MCS |
| 12 | 17 Jun 2016 | F1/T3 | 27.0 m s$^{-1}$ | 490 km | 6 | 3 | High | MCS |
| 13 | 2 Mar 2017 | F1/T2 | 30.0 m s$^{-1}$ | 860 km | 2 | 1 | Low | NCFR |
| 14 | 29 Jun 2017 | F1/T3 | 25.5 m s$^{-1}$ | 475 km | 2 | 0 | Moderate | MCS |
| 15 | 10 Aug 2017 | F1/T3 | — | 640 km | 1 | 0 | Moderate | MCS |
| 16 | 11 Aug 2017 | F1/T3 | 42.0 m s$^{-1}$ | 580 km | 26 | 6 | High | MCS |

[a] Damage rating assigned in Fujita and Torro scales, considering only the area of Poland.
[b] Considering only the area of Poland; peak wind gusts were derived from WMO ground-based observations.
[c] Distance between first and last damage report, considering the entire derecho life cycle also in other countries.

of thunderstorms over Poland (Kolendowicz 2006, 2012; Kolendowicz et al. 2017).

### e. Derechos

Derechos in Poland are generally rare events. In total, 16 derechos were detected over the course of 10 years (Table 5). Among all MCSs analyzed in this study, only 1.5% (and 9.1% among all QLCSs) evolved into derecho intensity. Warm-season derechos in Poland are more common and generate bigger impact than do their cold-season equivalent, the latter being mostly associated with NCFRs (Table 5; Fig. 11). However, as NCFRs move faster, damage tracks of cold-season derechos are significantly longer and in certain cases can exceed even 1000 km. The main direction from which cold-season derechos move is west-northwest, which is strictly related to trajectories of cold fronts over central Europe during wintertime. As indicated by Gatzen et al. (2020) cold-season derechos in Europe often start near the ''Benelux'' countries and travel eastwardly through Germany, the Czech Republic, Poland, and Slovakia. Warm-season derechos cover smaller areas but are mostly of moderate to high intensity, cause more deaths and injuries, and are capable of producing wind gusts up to 150 km h$^{-1}$ typically more often than cold-season derechos. On the radar scans they usually contain a well-developed bow echo pushed by a descending rear-inflow-jet (Fig. 11). Especially intense high-impact events inducing significant damage occurred on 23 July 2009 (Celiński-Mysław and Matuszko 2014) and 11 August 2017 (Taszarek et al. 2019). Unlike cold-season derechos, they mostly come from the south, south-southwest, and west-southwest directions, which is also in agreement with a derecho climatology for Germany (Gatzen et al. 2020). They usually develop over Germany and the Czech Republic and enter Poland in the late-afternoon hours. Only two cases (17 June 2016 and 29 June 2017) started over Poland.

The density of derecho events (derived from the spatial extent of each case) indicates that over the studied period the highest number of such systems took place over southwestern parts of the country and the lowest number occurred over the north (Fig. 11). In comparing this estimate with the derecho frequency over the United States (Coniglio et al. 2004), it is found that the density in Poland is lower by roughly a factor of 3 relative to the belt stretching from the southern Great Plains to the eastern part of the Midwest. The peak density of derechos in Poland is similar to that in the northern Great Plains.

## 4. Discussion and conclusions

In this work, a 10-yr climatology of MCSs and derechos was constructed for Poland. For the first time, a quantitative and qualitative analysis of MCS occurrence in this part of Europe has been derived from radar and lightning data, as contrasted with previous studies that were based on satellite images. All MCS cases were derived from a manual analysis (supported by an automated algorithm) and were clustered into spatial polygons. Identification of 766 cases allowed us to yield numerous conclusions, of which the most important are listed below:

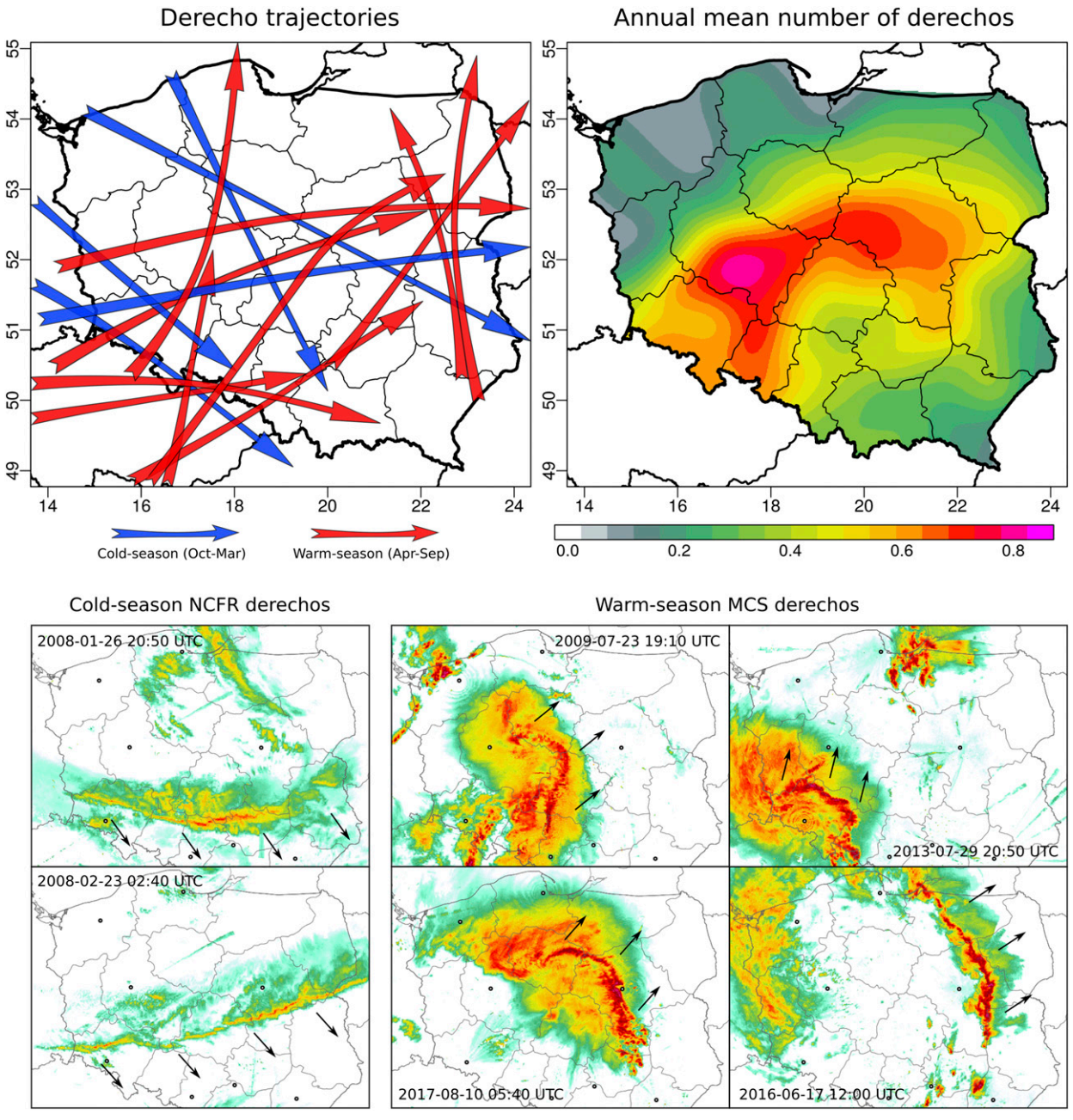


FIG. 11. (top left) Derecho trajectories and (top right) annual mean number of derechos. Derecho density was derived from the spatial extent of each case and by applying a 5 km × 5 km focal mean smoothing. (bottom) Example radar scans of cold-season NCFR and warm-season MCS derechos. Note that radar scans of other derechos (as listed in Table 5) are also provided in Figs. 1 and 2. Only cases from 2008 to 2017 and producing damage on the territory of Poland are taken into account.

1) MCS are not rare in Poland and can bring a serious impact to society and infrastructure when evolving into derecho intensity [e.g., 23 July 2009 (Celiński-Mysław and Matuszko 2014) and 11 August 2017 (Taszarek et al. 2019)] or being a result of significant supercells [e.g., 15 August 2008 (Taszarek and Gromadzki 2017) and 7 July 2017 (Poręba and Ustrnul 2020)]. An annual mean of 77 MCS cases and 49 days with MCS can be depicted for Poland.
2) The most frequent morphological MCS type is a broken line (58% of all MCSs; 44 per year), then areal/cluster (25%; 19) and squall/bow echo (17%; 13). Among QLCS as much as 72% (10 per year) are associated with a presence of a bow echo, which is

consistent with estimates by Celiński-Mysław and Palarz (2017). Precipitation archetypes considered within broken lines and QLCS yielded that trailing stratiform (73% of all linear MCSs; 42 per year) and parallel stratiform (25%; 14.4) types are the most common. Similar results were also obtained by Parker and Johnson (2000) for the United States.

3) Lifetime of a typical MCS in Poland ranges from 3 to 6 h, with initiation time around the afternoon hours (1200–1400 UTC) and dissipating stage in the evening (1900–2000 UTC). This result is consistent with Morel and Senesi (2002b) who indicated a mean MCS duration time from 5 to 8 h and peak developing time in the afternoon hours. QLCS in our database usually last longer than areal/clusters and broken lines and usually dissipate during nighttime hours.
4) The annual cycle in the occurrence of MCSs is consistent with the climatology of lightning over central Europe (Taszarek et al. 2015; Poelman et al. 2016; Enno et al. 2020), with a peak in mid-July. Enhanced MCS frequency is observed in the period from mid-May to late August, whereas during the cold season (October–March) MCSs are extremely rare. The cold season is dominated by NCFRs, but these systems usually do not meet MCS criteria. However, occasionally they can also reach derecho intensity.
5) For any specific location, the mean annual number of MCSs varies generally from 10 to 16, but, as evidenced over selected years, this value may range from only a few cases (2008) to as many as 27 (2017). A temporal shift in the MCS peak activity with early July over the southeast and late July/early August over the northwest was also found.
6) A majority of MCSs moves from the west, southwest, and south sectors, which is consistent with satellite-based estimates from Morel and Senesi (2002b). Only a minor fraction of MCSs propagate from other directions.
7) The majority of derechos in Poland were produced by a warm-season QLCS (9.1% of all QLCS and 1.5% of all MCS evolved into derechos). Four derechos were produced by cold-season NCFR systems and did not meet MCS criteria. Warm-season derechos in Poland (69% from all analyzed derechos) produced a bigger impact than did cold-season events, even though their damage paths were shorter [consistent with (Gatzen et al. 2020)]. Cold-season derechos moved predominantly from the west-northwest, whereas their warm-season equivalents moved from sectors ranging from west to south. The month with the highest number of derechos in Poland is July (31% from all analyzed derechos), which is consistent with Gatzen et al. (2020) but differs from the results obtained by Celiński-Mysław and Matuszko (2014) on a prior derecho climatology for Poland.

Our research, as one of the first attempts for a European country, provides a starting point for further work about radar-based climatology of MCSs. Such systems are a considerable source of precipitation during the warm season and play an important role in the hydroclimate of Europe, with implications for water availability and agriculture. This topic requires further attention to allow better understanding of how often and what types of MCSs occur over various parts of Europe and how big their influence on a water balance may be. Not without significance is the impact that they have on society and infrastructure by their potential for generating severe weather. Rapid development of radar networks across European countries and an increase in their measurement periods will allow an increasing number of similar studies in future. In future steps, we aim to expand the MCS database obtained in this study and compare classified archetypes with accompanying thermodynamic and kinematic conditions derived from proximity soundings and reanalysis data. This approach may lead to better understanding of MCS formation over Europe and potential improvements in their forecasting and the ability to anticipate associated threats such as heavy rainfall or severe wind gusts.

*Acknowledgments.* This research was supported by a grant from the Polish National Science Centre (Project 2017/27/B/ST10/00297) and a microgrant from the University of Warsaw. We thank EUCLID for providing lightning data and the Polish Institute of Meteorology and Water Management-National Research Institute for providing radar data.

## REFERENCES

Anderson, C. J., and R. W. Arritt, 1998: Mesoscale convective complexes and persistent elongated convective systems over the United States during 1992 and 1993. *Mon. Wea. Rev.*, **126**, 578–599, https://doi.org/10.1175/1520-0493(1998)126<0578:MCCAPE>2.0.CO;2.

Ashley, W. S., and T. L. Mote, 2005: Derecho hazards in the United States. *Bull. Amer. Meteor. Soc.*, **86**, 1577–1592, https://doi.org/10.1175/BAMS-86-11-1577.

——, ——, P. G. Dixon, S. L. Trotter, E. J. Powell, J. D. Durkee, and A. J. Grundstein, 2003: Distribution of mesoscale convective complex rainfall in the United States. *Mon. Wea. Rev.*, **131**, 3003–3017, https://doi.org/10.1175/1520-0493(2003)131<3003:DOMCCR>2.0.CO;2.

Augustine, J. A., and K. W. Howard, 1988: Mesoscale convective complexes over the United States during 1985. *Mon. Wea. Rev.*,**116**, 685–701, https://doi.org/10.1175/1520-0493(1988)116<0685:MCCOTU>2.0.CO;2.

Bartels, D. L., and R. A. Maddox, 1991: Midlevel cyclonic vortices generated by mesoscale convective systems. *Mon. Wea. Rev.*, **119**, 104–118, https://doi.org/10.1175/1520-0493(1991)119<0104:MCVGBM>2.0.CO;2.

Bentley, M. L., and T. L. Mote, 1998: A climatology of derecho-producing mesoscale convective systems in the central and eastern United States, 1986–95. Part I: Temporal and spatial distribution. *Bull. Amer. Meteor. Soc.*, **79**, 2527–2540, https://doi.org/10.1175/1520-0477(1998)079<2527:ACODPM>2.0.CO;2.

——, and J. A. Sparks, 2003: A 15 yr climatology of derecho-producing mesoscale convective systems over the central and eastern United States. *Climate Res.*, **24**, 129–139, https://doi.org/10.3354/cr024129.

Bielec-Bąkowska, Z., 2003: Long-term variability of thunderstorm occurrence in Poland in the 20th century. *Atmos. Res.*, **67–68**, 35–52, https://doi.org/10.1016/S0169-8095(03)00082-6.

Blanchard, D. O., 1990: Mesoscale convective patterns of the southern High Plains. *Bull. Amer. Meteor. Soc.*, **71**, 994–1005, https://doi.org/10.1175/1520-0477(1990)071<0994:MCPOTS>2.0.CO;2.

Bluestein, H. B., and M. H. Jain, 1985: Formation of mesoscale lines of precipitation: Severe squall lines in Oklahoma during the spring. *J. Atmos. Sci.*, **42**, 1711–1732, https://doi.org/10.1175/1520-0469(1985)042<1711:FOMLOP>2.0.CO;2.

Bosart, L. F., and F. Sanders, 1981: The Johnstown flood of July 1977: A long-lived convective system. *J. Atmos. Sci.*, **38**, 1616–1642, https://doi.org/10.1175/1520-0469(1981)038<1616:TJFOJA>2.0.CO;2.

Burke, P. C., and D. M. Schultz, 2004: A 4-yr climatology of cold-season bow echoes over the continental United States. *Wea. Forecasting*, **19**, 1061–1074, https://doi.org/10.1175/811.1.

Celiński-Mysław, D., and D. Matuszko, 2014: An analysis of selected cases of derecho in Poland. *Atmos. Res.*, **149**, 263–281, https://doi.org/10.1016/j.atmosres.2014.06.016.

——, and A. Palarz, 2017: The occurrence of convective systems with a bow echo in warm season in Poland. *Atmos. Res.*, **193**, 26–35, https://doi.org/10.1016/j.atmosres.2017.04.015.

——, ——, and Ł. Łoboda, 2019: Kinematic and thermodynamic conditions related to convective systems with a bow echo in Poland. *Theor. Appl. Climatol.*, **137**, 2109–2123, https://doi.org/10.1007/s00704-018-2728-6.

——, ——, and M. Taszarek, 2020: Climatology and atmospheric conditions associated with cool season bow echo storms in Poland. *Atmos. Res.*, **240**, 104944, https://doi.org/10.1016/j.atmosres.2020.104944.

Chumchean, S., A. Seed, and A. Sharma, 2004: Application of scaling in radar reflectivity for correcting range-dependent bias in climatological radar rainfall estimates. *J. Atmos. Oceanic Technol.*, **21**, 1545–1556, https://doi.org/10.1175/1520-0426(2004)021<1545:AOSIRR>2.0.CO;2.

Cohen, A. E., M. C. Coniglio, S. F. Corfidi, and S. J. Corfidi, 2007: Discrimination of mesoscale convective system environments using sounding observations. *Wea. Forecasting*, **22**, 1045–1062, https://doi.org/10.1175/WAF1040.1.

Coniglio, M. C., D. J. Stensrud, and M. B. Richman, 2004: An observational study of derecho-producing convective systems. *Wea. Forecasting*, **19**, 320–337, https://doi.org/10.1175/1520-0434(2004)019<0320:AOSODC>2.0.CO;2.

——, J. Y. Hwang, and D. J. Stensrud, 2010: Environmental factors in the upscale growth and longevity of MCSs derived from rapid update cycle analyses. *Mon. Wea. Rev.*, **138**, 3514–3539, https://doi.org/10.1175/2010MWR3233.1.

Doswell, C. A., H. E. Brooks, and R. A. Maddox, 1996: Flash flood forecasting: An ingredients-based methodology. *Wea. Forecasting*, **11**, 560–581, https://doi.org/10.1175/1520-0434(1996)011<0560:FFFAIB>2.0.CO;2.

Dotzek, N., P. Groenemeijer, B. Feuerstein, and A. M. Holzer, 2009: Overview of ESSL's severe convective storms research using the European Severe Weather Database ESWD. *Atmos. Res.*, **93**, 575–586, https://doi.org/10.1016/j.atmosres.2008.10.020.

Enno, S. E., J. Sugier, R. Alber, and M. Seltzer, 2020: Lightning flash density in Europe based on 10 years of ATDnet data. *Atmos. Res.*, **235**, 104769, https://doi.org/10.1016/j.atmosres.2019.104769.

Evans, J. S., and C. A. Doswell III, 2001: Examination of derecho environments using proximity soundings. *Wea. Forecasting*, **16**, 329–342, https://doi.org/10.1175/1520-0434(2001)016<0329:EODEUP>2.0.CO;2.

Fiolleau, T., and R. Roca, 2013: An algorithm for the detection and tracking of tropical mesoscale convective systems using infrared images from geostationary satellite. *IEEE Trans. Geosci. Remote Sens.*, **51**, 4302–4315, https://doi.org/10.1109/TGRS.2012.2227762.

Fritsch, J. M., and G. S. Forbes, 2001: Mesoscale convective systems. Severe Convective Storms, Meteor. Monogr., No. 50, Amer. Meteor. Soc., 323–358.

——, R. J. Kane, and C. R. Chelius, 1986: The contribution of mesoscale convective weather systems to the warm-season precipitation in the United States. *J. Climate Appl. Meteor.*, **25**, 1333–1345, https://doi.org/10.1175/1520-0450(1986)025<1333:TCOMCW>2.0.CO;2.

Fujita, T. T., 1971: Proposed characterization of tornadoes and hurricanes by area and intensity. University of Chicago SMRP Research Paper Vol. 91, 45 pp.

Gallus, W. A., N. A. Snook, and E. V. Johnson, 2008: Spring and summer severe weather reports over the midwest as a function of convective mode: A preliminary study. *Wea. Forecasting*, **23**, 101–113, https://doi.org/10.1175/2007WAF2006120.1.

Gatzen, C., 2011: A 10-year climatology of cold-season narrow cold-frontal rainbands in Germany. *Atmos. Res.*, **100**, 366–370, https://doi.org/10.1016/j.atmosres.2010.09.018.

——, A. H. Fink, D. M. Schulz, and J. G. Pinto, 2020: An 18-year climatology of derechos in Germany. *Nat. Hazards Earth Syst. Sci.*, **20**, 1335–1351, https://doi.org/10.5194/nhess-20-1335-2020.

Geerts, B., 1998: Mesoscale convective systems in the southeast United States during 1994–95: A survey. *Wea. Forecasting*, **13**, 860–869, https://doi.org/10.1175/1520-0434(1998)013<0860:MCSITS>2.0.CO;2.

Gospodinov, I., T. Dimitrova, L. Bocheva, P. Simeonov, and R. Dimitrov, 2015: Derecho-like event in Bulgaria on 20 July 2011. *Atmos. Res.*, **158–159**, 254–273, https://doi.org/10.1016/j.atmosres.2014.05.009.

Guastini, C. T., and L. F. Bosart, 2016: Analysis of a progressive derecho climatology and associated formation environments. *Mon. Wea. Rev.*, **144**, 1363–1382, https://doi.org/10.1175/MWR-D-15-0256.1.

Haberlie, A. M., and W. S. Ashley, 2018a: A method for identifying mesoscale convective systems in radar mosaics. Part I: Segmentation and classification. *J. Appl. Meteor. Climatol.*, **57**, 1575–1598, https://doi.org/10.1175/JAMC-D-17-0293.1.

——, and ——, 2018b: A method for identifying midlatitude mesoscale convective systems in radar mosaics. Part II: Tracking. *J. Appl. Meteor. Climatol.*, **57**, 1599–1621, https://doi.org/10.1175/JAMC-D-17-0294.1.

——, and ——, 2019: A radar-based climatology of mesoscale convective systems in the United States. *J. Climate*, **32**, 1591–1606, https://doi.org/10.1175/JCLI-D-18-0559.1.

Hamid, K., 2012: Investigation of the passage of the derecho in Belgium. *Atmos. Res.*, **107**, 86–105, https://doi.org/10.1016/j.atmosres.2011.12.013.

He, Z. W., Q. H. Zhang, and J. Sun, 2016: The contribution of mesoscale convective systems to intense hourly precipitation events during the warm seasons over central East China. *Adv. Atmos. Sci.*, **33**, 1233–1239, https://doi.org/10.1007/s00376-016-6034-x.

Hobbs, P. V., and K. R. Biswas, 1979: The cellular structure of narrow cold-frontal rainbands. *Quart. J. Roy. Meteor. Soc.*, **105**, 723–727, https://doi.org/10.1002/qj.49710544516.

Houze, R. A., 2004: Mesoscale convective systems. *Rev. Geophys.*, **42**, RG4003, https://doi.org/10.1029/2004RG000150.

——, 2019: 100 years of research on mesoscale convective systems. *A Century of Progress in Atmospheric and Related Sciences: Celebrating the American Meteorological Society Centennial, Meteor. Monogr.*, No. 59, https://doi.org/10.1175/AMSMONOGRAPHS-D-18-0001.1.

Houze, R. A., Jr., 1993: *Cloud Dynamics*. Academic Press, 573 pp.

Jirak, I. L., W. R. Cotton, and R. L. McAnelly, 2003: Satellite and radar survey of mesoscale convective system development. *Mon. Wea. Rev.*, **131**, 2428–2449, https://doi.org/10.1175/1520-0493(2003)131<2428:SARSOM>2.0.CO;2.

Johns, R. H., and W. D. Hirt, 1987: Derechos: Widespread convectively induced windstorms. *Wea. Forecasting*, **2**, 32–49, https://doi.org/10.1175/1520-0434(1987)002<0032:DWCIW>2.0.CO;2.

Jurczyk, A., K. Osródka, and J. Szturc, 2008: Research studies on improvement in real-time estimation of radar-based precipitation in Poland. *Meteor. Atmos. Phys.*, **101**, 159–173, https://doi.org/10.1007/s00703-007-0266-3.

Klimowski, B. A., M. R. Hjelmfelt, and M. J. Bunkers, 2004: Radar observations of the early evolution of bow echoes. *Wea. Forecasting*, **19**, 727–734, https://doi.org/10.1175/1520-0434(2004)019<0727:ROOTEE>2.0.CO;2.

Koch, S. E., and P. J. Kocin, 1991: Frontal contraction processes leading to the formation of an intense narrow rainband. *Meteor. Atmos. Phys.*, **46**, 123–154, https://doi.org/10.1007/BF01027339.

Kolendowicz, L., 2006: The influence of synoptic situations on the occurrence of days with thunderstorms during a year in the territory of Poland. *Int. J. Climatol.*, **26**, 1803–1820, https://doi.org/10.1002/joc.1348.

——, 2012: Synoptic patterns associated with thunderstorms in Poland. *Meteor. Z.*, **21**, 145–156, https://doi.org/10.1127/0941-2948/2012/0272.

——, M. Taszarek, and B. Czernecki, 2017: Atmospheric circulation and sounding-derived parameters associated with thunderstorm occurrence in central Europe. *Atmos. Res.*, **191**, 101–114, https://doi.org/10.1016/j.atmosres.2017.03.009.

Kolios, S., and H. Feidas, 2010: A warm season climatology of mesoscale convective systems in the Mediterranean basin using satellite data. *Theor. Appl. Climatol.*, **102**, 29–42, https://doi.org/10.1007/s00704-009-0241-7.

Lewis, M. W., and S. L. Gray, 2010: Categorisation of synoptic environments associated with mesoscale convective systems over the UK. *Atmos. Res.*, **97**, 194–213, https://doi.org/10.1016/j.atmosres.2010.04.001.

Loehrer, S. M., and R. H. Johnson, 1995: Surface pressure and precipitation life cycle characteristics of PRE-STORM mesoscale convective systems. *Mon. Wea. Rev.*, **123**, 600–621, https://doi.org/10.1175/1520-0493(1995)123<0600:SPAPLC>2.0.CO;2.

Maddox, R. A., 1980: Mesoscale convective complexes. *Bull. Amer. Meteor. Soc.*, **61**, 1374–1387, https://doi.org/10.1175/1520-0477(1980)061<1374:MCC>2.0.CO;2.

Markowski, P., and Y. Richardson, 2010: Mesoscale convective systems. *Mesoscale Meteorology in Midlatitudes*, P. Markowski and Y. Richardson, Eds., John Wiley and Sons, 245–272.

Mathias, L., V. Ermert, F. D. Kelemen, P. Ludwig, and J. G. Pinto, 2017: Synoptic analysis and hindcast of an intense bow echo in western Europe: The 9 June 2014 storm. *Wea. Forecasting*, **32**, 1121–1141, https://doi.org/10.1175/WAF-D-16-0192.1.

——, P. Ludwig, and J. G. Pinto, 2019: Synoptic-scale conditions and convection-resolving hindcast experiments of a cold-season derecho on 3 January 2014 in western Europe. *Nat. Hazards Earth Syst. Sci.*, **19**, 1023–1040, https://doi.org/10.5194/nhess-19-1023-2019.

Meaden, G. T., 1976: Tornadoes in Britain: Their intensities and distribution in space and time. *J. Meteor.*, **1**, 242–251.

Moore, B. J., P. J. Neiman, F. M. Ralph, and F. E. Barthold, 2012: Physical processes associated with heavy flooding rainfall in Nashville, Tennessee, and vicinity during 1–2 May 2010: The role of an atmospheric river and mesoscale convective systems. *Mon. Wea. Rev.*, **140**, 358–378, https://doi.org/10.1175/MWR-D-11-00126.1.

Morel, C., and S. Senesi, 2002a: A climatology of mesoscale convective systems over Europe using satellite infrared imagery. I: Methodology. *Quart. J. Roy. Meteor. Soc.*, **128**, 1953–1971, https://doi.org/10.1256/003590002320603485.

——, and ——, 2002b: A climatology of mesoscale convective systems over Europe using satellite infrared imagery. II: Characteristics of European mesoscale convective systems. *Quart. J. Roy. Meteor. Soc.*, **128**, 1973–1995, https://doi.org/10.1256/003590002320603494.

Nolen, R. H., 1959: A radar pattern associated with tornadoes. *Bull. Amer. Meteor. Soc.*, **40**, 277–279, https://doi.org/10.1175/1520-0477-40.6.277.

Ośródka, K., J. Szturc, and A. Jurczyk, 2014: Chain of data quality algorithms for 3-D single-polarization radar reflectivity (RADVOL-QC system). *Meteor. Appl.*, **21**, 256–270, https://doi.org/10.1002/met.1323.

Parker, M. D., and R. H. Johnson, 2000: Organizational modes of midlatitude mesoscale convective systems. *Mon. Wea. Rev.*, **128**, 3413–3436, https://doi.org/10.1175/1520-0493(2001)129<3413:OMOMMC>2.0.CO;2.

Peters, J. M., and R. S. Schumacher, 2014: Objective categorization of heavy-rain-producing MCS synoptic types by rotated principal component analysis. *Mon. Wea. Rev.*, **142**, 1716–1737, https://doi.org/10.1175/MWR-D-13-00295.1.

Pinto, J. O., J. A. Grim, and M. Steiner, 2015: Assessment of the High-Resolution Rapid Refresh model's ability to predict mesoscale convective systems using object-based evaluation. *Wea. Forecasting*, **30**, 892–913, https://doi.org/10.1175/WAF-D-14-00118.1.

Poelman, D. R., W. Schulz, G. Diendorfer, and M. Bernardi, 2016: The European lightning location system EUCLID—Part 2: Observations. *Nat. Hazards Earth Syst.*, **16**, 607–616, https://doi.org/10.5194/nhess-16-607-2016.

Poręba, S., and Z. Ustrnul, 2020: Forecasting experiences associated with supercells over South-Western Poland on July 7, 2017. *Atmos. Res.*, **232**, 104681, https://doi.org/10.1016/j.atmosres.2019.104681.

Punkka, A.-J., and M. Bister, 2005: Occurrence of summertime convective precipitation and mesoscale convective systems in Finland 2000–01. *Mon. Wea. Rev.*, **133**, 362–373, https://doi.org/10.1175/MWR-2854.1.

——, and ——, 2015: Mesoscale convective systems and their synoptic-scale environment in Finland. *Wea. Forecasting*, **30**, 182–196, https://doi.org/10.1175/WAF-D-13-00146.1.

R Core Team, 2013: R: A language and environment for statistical computing. R Foundation, Vienna, Austria, accessed 1 December 2019, https://www.r-project.org/.

Rigo, T., and M. C. Llasat, 2004: A methodology for the classification of convective structures using meteorological radar: Application to heavy rainfall events on the Mediterranean coast of the Iberian Peninsula. *Nat. Hazards Earth Syst. Sci.*, **4**, 59–68, https://doi.org/10.5194/nhess-4-59-2004.

——, and ——, 2007: Analysis of mesoscale convective systems in Catalonia using meteorological radar for the period 1996–2000. *Atmos. Res.*, **83**, 458–472, https://doi.org/10.1016/j.atmosres.2005.10.016.

Rotunno, R., J. B. Klemp, and M. L. Weisman, 1988: A theory for strong, long-lived squall lines. *J. Atmos. Sci.*, **45**, 463–485, https://doi.org/10.1175/1520-0469(1988)045<0463:ATFSLL>2.0.CO;2.

Salio, P., M. Nicolini, and E. J. Zipser, 2007: Mesoscale convective systems over southeastern South America and their relationship with the South American low-level jet. *Mon. Wea. Rev.*, **135**, 1290–1309, https://doi.org/10.1175/MWR3305.1.

Schulz, W., G. Diendorfer, S. Pedeboy, and D. R. Poelman, 2016: The European lightning location system EUCLID—Part 1: Performance analysis and validation. *Nat. Hazards Earth Syst. Sci.*, **16**, 595–605, https://doi.org/10.5194/nhess-16-595-2016.

Schumacher, R. S., and R. H. Johnson, 2005: Organization and environmental properties of extreme-rain-producing mesoscale convective systems. *Mon. Wea. Rev.*, **133**, 961–976, https://doi.org/10.1175/MWR2899.1.

——, and ——, 2006: Characteristics of U.S. extreme rain events during 1999–2003. *Wea. Forecasting*, **21**, 69–85, https://doi.org/10.1175/WAF900.1.

——, and ——, 2008: Mesoscale processes contributing to extreme rainfall in a midlatitude warm-season flash flood. *Mon. Wea. Rev.*, **136**, 3964–3986, https://doi.org/10.1175/2008MWR2471.1.

——, and ——, 2009: Quasi-stationary, extreme-rain-producing convective systems associated with midlevel cyclonic circulations. *Wea. Forecasting*, **24**, 555–574, https://doi.org/10.1175/2008WAF2222173.1.

Siwek, G. M., 2016: Charakterystyka wezbrania opadowego w zlewni górnego Wieprza w maju 2014 roku. *Ann. UMCS*, **71B**, 45–59, https://doi.org/10.17951/b.2016.71.1.45.

Taszarek, M., and J. Gromadzki, 2017: Deadly tornadoes in Poland from 1820 to 2015. *Mon. Wea. Rev.*, **145**, 1221–1243, https://doi.org/10.1175/MWR-D-16-0146.1.

——, B. Czernecki, and A. Kozioł, 2015: A cloud-to ground lightning climatology for Poland. *Mon. Wea. Rev.*, **143**, 4285–4304, https://doi.org/10.1175/MWR-D-15-0206.1.

——, H. E. Brooks, B. Czernecki, P. Szuster, and K. Fortuniak, 2018: Climatological aspects of convective parameters over Europe: A comparison of ERA-Interim and sounding data. *J. Climate*, **31**, 4281–4308, https://doi.org/10.1175/JCLI-D-17-0596.1.

——, and Coauthors, 2019: Derecho evolving from a mesocyclone—A study of 11 August 2017 severe weather outbreak in Poland: Event analysis and high-resolution simulation. *Mon. Wea. Rev.*, **147**, 2283–2306, https://doi.org/10.1175/MWR-D-18-0330.1.

Terti, G., I. Ruin, S. Anquetin, and J. J. Gourley, 2017: A situation-based analysis of flash flood fatalities in the United States. *Bull. Amer. Meteor. Soc.*, **98**, 333–345, https://doi.org/10.1175/BAMS-D-15-00276.1.

Toll, V., A. Männik, A. Luhmaa, and R. Rõõm, 2015: Hindcast experiments of the derecho in Estonia on 08 August, 2010: Modeling derecho with NWP model HARMONIE. *Atmos. Res.*, **158–159**, 179–191, https://doi.org/10.1016/j.atmosres.2014.10.011.

Trapp, R. J., S. A. Tessendorf, E. S. Godfrey, and H. E. Brooks, 2005: Tornadoes from squall lines and bow echoes. Part I: Climatological distribution. *Wea. Forecasting*, **20**, 23–34, https://doi.org/10.1175/WAF-835.1.

Velasco, I. Y., and J. M. Fritsch, 1987: Mesoscale convective complexes in the Americas. *J. Geophys. Res.*, **92**, 9591–9613, https://doi.org/10.1029/JD092iD08p09591.

Walczakiewicz, S., and K. Ostrowski, 2010: Nawałnica z 4 VII 2002 r. jako przykład bow echo w Europie Środkowo-Wschodniej ze szczególnym uwzględnieniem burzy w Puszczy Piskiej (The storm of 4 July 2002 as an example of bow echo in central and eastern Europe, with particular emphasis on the storm in the Pisz Forest). *Geo-Sympozjum Młodych Badaczy Silesia 2010*, Bytom, Poland, University of Silesia Faculty of Earth Sciences, 213–230.

Weisman, M. L., and R. Rotunno, 2004: "A theory for strong long-lived squall lines" revisited. *J. Atmos. Sci.*, **61**, 361–382, https://doi.org/10.1175/1520-0469(2004)061<0361:ATFSLS>2.0.CO;2.

Widawski, A., and W. Pilorz, 2018: The Mesoscale Convective Systems with bow echo radar signatures as an example of extremely severe and widespread geohazard in Poland. *Environ. Socio-Economic Stud.*, **6**, 10–16, https://doi.org/10.2478/environ-2018-0002.

Yang, X. R., J. F. Fei, X. G. Huang, X. P. Cheng, L. W. V. Carvalho, and H. R. He, 2015: Characteristics of mesoscale convective systems over China and its vicinity using geostationary satellite FY2. *J. Climate*, **28**, 4890–4907, https://doi.org/10.1175/JCLI-D-14-00491.1.

Zhang, L., J. Min, X. Zhuang, and R. Schumacher, 2019: General features of extreme rainfall events produced by MCSs over east China during 2016–17. *Mon. Wea. Rev.*, **147**, 2693–2714, https://doi.org/10.1175/MWR-D-18-0455.1.

Zheng, L., J. Sun, X. Zhang, and C. Liu, 2013: Organizational modes of mesoscale convective systems over central east China. *Wea. Forecasting*, **28**, 1081–1098, https://doi.org/10.1175/WAF-D-12-00088.1.